Available online at www.sciencedirect.com
SCIENCE DIRECT®
International Journal of Heat and Mass Transfer 48 (2005) 4953–4962
International Journal of HEAT and MASS TRANSFER
www.elsevier.com/locate/ijhmt

Heat and mass transfer during silica gel–moisture interactions

Jin Sun *, Robert W. Besant

Department of Mechanical Engineering, University of Saskatchewan, 57 Campus Drive, Saskatoon, SK, Canada S7N 5A9

Received 30 January 2004; received in revised form 7 January 2005
Available online 18 August 2005

Abstract

An initially dry granular silica gel bed is subject to a sudden uniform air flow at a selected temperature and humidity. The coupled non-equilibrium heat transfer and moisture transfer were investigated experimentally and numerically. This study provides a fundamental view of heat and mass transfer process within the granular particle pores. It was found that only a small fraction of internal surface area of silica gel is exposed to water vapour during the test and this occurs very slowly with a time delay that must be accounted for in the model. This modified model gives transient response results that agree with the experimental data within the uncertainty bounds.

Keywords: Silica gel; Water vapour; Adsorption; Heat and mass transfer; Specific surface area

1. Introduction

For the last two decades, silica gel (SiO_2) has been used as a high performance desiccant to remove water vapour from humid ventilation air for buildings [1]. It has very high moisture adsorption capacity because of its microporous structure of internal interlocking cavities which gives a high internal surface area (up to 800 m^2/g, or 10^{-8}–10^{-9} m^2/m^3) [2]. When the water vapour pressure at or near any pore region of a silica gel particle is lower than the adjacent air water vapour pressure, water molecules diffuse through the air to the surface and adhere to the surfaces, especially the internal surface of the silica gel particles. The higher the humidity of the air, the greater the mass of the water adsorbed by the silica gel. There is no chemical reaction during adsorption. Even when saturated with water vapour, silica gel still has the appearance of a dry product with its shape unchanged. The adsorption and desorption characteristics of different silica gel samples may vary because of different manufacturing procedures [3]. Although silica gel has been frequently used as desiccant, the detailed heat and moisture transfer process within the pores of silica gel particles is not completely understood as research is on going.

San and Jiang [4] tested and analytically modeled a packed-bed silica gel dehumidification system. Based on the assumption of solid-side resistance method [2] and using several non-dimensional variables, they analyzed the heat and mass transfer process in the system at different temperatures. Fujii and Lior [5] developed a transient two-dimensional numerical model. The heat and mass transfer between a humid laminar air stream and a solid parallel desiccant bed were conjugated. In

* Corresponding author.
E-mail address: jis396@mail.usask.ca (J. Sun).

0017-9310/$ - see front matter © 2005 Elsevier Ltd. All rights reserved.
doi:10.1016/j.ijheatmasstransfer.2005.02.043

Nomenclature

B_{im}	Biot number for mass transfer
c_p	specific heat at constant pressure [J/(kg K)]
d_p	diameter of silica gel particle (m)
D_i	internal diffusion coefficient (m^2/s)
D_v	vapour/air mutual diffusivity (m^2/s)
$D_{v,eff}$	effective air/vapour mutual diffusivity (m^2/s)
G_γ	mass flux [kg/(m^2 s)]
h_{m_0}	convective mass transfer coefficient (m/s)
$h_{\sigma\gamma}$	internal heat convection coefficient [W/(m^2 K)]
H_{fg}	latent heat of condensation (J/kg)
J_d	Chilton and Colburn mass transfer factor
J_h	Chilton and Colburn heat convection factor
k	thermal conductivity [W/(m K)]
k_{eff}	effective thermal conductivity [W/(m K)]
k_g	internal mass transfer coefficient [kg/(m^2 Pa s)]
K	permeability of silica gel sample (m^2)
L	thickness of the silica gel sample bed (m)
m	mass (kg)
$\dot{m}$	mass flow rate (kg/s)
M_a	molecular weight of gas (g/mol)
P	pressure (Pa)
Pr	Prandtl number of gas
P_{vs}	partial pressure of the water vapour in a saturated mixture (Pa)
Q	moisture–silica gel heat effect (J/kg)
r	radius (m)
r_h	hydraulic radius of the porous medium (m)
$\dot{r}_v$	water vapour adsorption rate [kg/(m^3 s)]
Re	Reynolds number of the air flow in the sample bed
RH	relative humidity (%)
Sc	Schmidt number
S_v	volume specific surface area of silica gel sample (m^2/m^3)
t	time (s)
T	temperature (K)
U_D	Darcy velocity (m/s)
V	volume (m^3)
W_v	humidity ratio of gas (kg/kg)
x	distance from the top of the sample bed (m)
X	moisture content of the silica gel particles (%)

Greek symbols

β	eigenvalues
ε	porosity of the silica gel sample; volume fraction
μ	air dynamic viscosity (kg/m s)
ν	air kinematics viscosity (m^2/s)
ρ	density (kg/m^3)
τ	tortuosity
ϕ	relative humidity of the gas at certain point in the sample bed
φ_w	relative humidity on the aqueous solution/air interface
Ω_β	volume change of aqueous solution layer per unit mass of moisture (m^3/kg)

Subscripts

0	initial
a	dry air
v	water vapour
β	liquid
γ	gas (dry air + water vapour)
σ	solid
∞	inlet

this model, an empirical correlation was used without considering the specific surface area of desiccant, to calculate the water adsorption rate. The numerical model demonstrated that the conjugated method produced less error in thick-bed (i.e., order of 2 cm) desiccant systems compared to conventional, non-conjugated method. However, no experimental data were presented to verify the model. Based on the work of Fujii and Lior, Al-Sharqawi and Lior [6] proposed an improved model by further considering a turbulent air stream flowing through a parallel desiccant bed. Both the laminar and turbulent air-stream models of the work were conjugate-transient two-dimensional numerical models without considering the specific surface area as an important variable. Ni and San [7] analytically investigated diffusion and adsorption within a microporous spherical particle subject to a constant internal diffusion coefficient, external convection heat and mass transfer coefficients employing the equilibrium adsorption isotherm assumption. The linear governing equations were solved and results were presented for selected values of dimensionless constants for uniform internal adsorbent temperatures. Peng et al. [8] tested and modeled the adsorption and dissolution process due to air flow through granular potash beds at non-equilibrium conditions. They built a one-dimensional transient heat and mass transfer model in which the specific surface area was assumed constant in calculation of water vapour adsorption rate. They found that non-equilibrium internal moisture and heat transfer processes can exist with significant property differences between the interstitial bed pore air and the potash particles.

In this paper, a transient, non-linear, one-dimensional numerical model was presented to investigate the cou-

pled moisture transfer and non-equilibrium heat transfer when humid air flowed through a bed of initially dry silica gel particles. Compared to the open literature, further improvement of the authors' model was made by attaching much importance on the specific surface area in the calculation of water adsorption rate by assuming it was exponentially time-dependent. This assumption is verified by good agreement between the simulation results and experimental data tested at different inlet air relative humidity conditions for two silica gel particle sizes.

2. Numerical simulation

The following assumptions are made in the development of the model: (1) the air flow passing through the silica gel bed is one-dimensional and steady; (2) the transport processes within the silica gel bed are transient convection and diffusion of heat and water vapour; (3) inside the macroscopic pore spaces of the particle bed, the gas phase is treated as an ideal gas mixture, the dry air and water vapour have one unique temperature at any point; the solid silica gel particles and adsorbed liquid water phase are assumed to be in a local thermodynamic equilibrium state that is not necessarily equal to the gaseous phase equilibrium state at the same point in the bed; (4) there is no water mobility, solid dissolution and chemical reactions taking place in the silica gel bed; (5) the internal surface area available for adsorption inside each silica gel particle within the bed increases with time as the water vapour slowly diffuses into each particle at a rate that is much slower than the rate of water vapour diffusion through air; (6) the porous medium properties of the particle bed are homogeneous and isotropic except for the latent heat of adsorption term; (7) $c_{p\gamma}$, $c_{p\sigma}$, μ, v, k_γ, k_σ, U_D, ρ_σ, ρ_β, ε_σ and D_v are assumed to be constant; (8) there is no particle movement in the bed during a test; (9) the initial condition of the silica gel particles is considered to be totally dry; (10) the local total gaseous pressure inside the pore space is assumed equal to the standard atmosphere pressure at any time.

Assumption 5 above implies a quasi-equilibrium condition for the adsorbed water at any time. To account for this time growth in available internal surface area at any point in the bed the diffusion process inside one spherical particle is first considered. For a particle of radius, r_0, subject to an internal water vapour diffusion process within the particle and the internal diffusion process rate is controlled by an internal diffusion coefficient, D_i, which is assumed to be constant and much smaller than the diffusion coefficient for water vapour in air, then the partial differential equation governing this vapour diffusion of internal particle is [9]:

$$\frac{\partial \rho_v}{\partial t} = \frac{D_i}{r^2} \cdot \frac{\partial}{\partial r}\left(r^2 \cdot \frac{\partial \rho_v}{\partial r}\right) \tag{1}$$

where the symbols are defined in the nomenclature. For a step change in the external vapour density, ρ_{v0}, from the initial condition, ρ_{vi}, the solution of Eq. (1) can be shown to be

$$\theta = \frac{\rho_v - \rho_{v0}}{\rho_{vi} - \rho_{v0}} = \sum_{i=1}^{\infty} C_i \cdot \frac{r_0}{r \cdot \beta_i} \cdot e^{-\beta_i^2 D_i t / r_0^2} \cdot \sin(\beta_i r / r_0) \tag{2}$$

where

$$C_i = \frac{4(\sin(\beta_i) - \beta_i(\sin\beta_i))}{2\beta_i - \sin(2\beta_i)} \tag{3}$$

and the eigenvalues, β_i, are found from the roots of the equation:

$$1 - \beta_i \cdot \cos(\beta_i) = B_{im} = h_{m_0} r_0 / D_i \tag{4}$$

In this equation, the mass transfer Biot number, B_{im}, is the ratio of the resistance of internal diffusion to external convective mass transfer resistance and h_{m_0} is the external surface convective mass transfer coefficient at $r = r_0$. This analytical solution is restricted to the case of the vapour density or partial pressure external to the particle undergoing a single step change at time $t = 0$. After time, $t^* = \frac{t \cdot D_i}{r_0^2} > 0.2$, the ratio of total mass of water vapour accumulated inside the spherical particle at any time, t, relative to the maximum gain at $t \to \infty$ will be

$$\frac{m}{m_0} = \frac{\int_{v_0}(\rho_v - \rho_{vi})\,dV}{(\rho_{vi} - \rho_{v0})V_0} = \frac{1}{V_0}\int_{V_0}(1-\theta)\,dV \tag{5}$$

$$= 1 - 3 \cdot C_1 \cdot e^{-\beta_i^2 t^*}\left[\frac{\sin\beta_1 - \beta_1\cos\beta_1}{\beta_1^3}\right] \tag{6}$$

where $0 < \beta_i(B_{im}) < 3.14$ and $1.0 < C_1(B_{im}) < 2.0$.

When $B_{im} > 100$, $\beta_1 = 3.14$ and $C_1 = 2.0$, then Eq. (6) becomes:

$$\frac{m}{m_0} = 1 + 0.6085\exp(-t/0.1014) \tag{7}$$

Furthermore, if we assume that this mass accumulation of water vapour by internal surface adsorption on each particle is directly proportional to the area of surface [10], then the apparent surface area per unit volume available for adsorption will grow with time, as implied by (6) or (7), such that the specific surface area inside each particle at each point in the bed can be written as

$$S_v = S_{v0} + S_{v1}(1 - e^{-t/t_0}) \tag{8}$$

Both S_{v1} and t_0 will depend in part on the initial humidity step size for a transient step change.

The adsorption rate of water vapour, $\dot{r}_v$, is a key variable which controls the heat transfer process during the silica gel–moisture interactions. The calculation of $\dot{r}_v$ is described using the formulation of Peng et al. [8], where the flux is directly proportional to the specific surface area and the difference between the vapour pressure in

the gaseous phase and the vapour pressure at the surface of the particles.

$$\dot{r}_v = k_g \cdot S_v \cdot [P_v - \phi_w \cdot P_{vs(T\sigma)}] \tag{9}$$

The constant of proportionality for gas vapour diffusion in (9) is expressed using the correlation:

$$k_g = \frac{J_d \cdot G_\gamma}{M_a \cdot P_a \cdot Sc^{2/3}} \tag{10}$$

where

$$G_\gamma = \rho_\gamma \cdot U_D/\varepsilon_\gamma \tag{11}$$

$$J_d = 0.048 \cdot Re^{-0.3} \tag{12}$$

where

$$Re = 4 \cdot r_h \cdot G_\gamma/\mu \tag{13}$$

where

$$r_h = \varepsilon_\gamma/S_v \tag{14}$$

The relative humidity on the aqueous solution/air interface, ϕ_w, in Eq. (9) is a function of moisture content X, and was generated by curve fitting the experimental data of moisture adsorption capacity measurement of silica gel particles at equilibrium conditions for moisture content increasing.

$$\phi_w = 0.0878 \cdot (100X)^3 - 1.5397 \cdot (100X)^2 + 10.931 \cdot (100X) \tag{15}$$

which has a curve fit, $R^2 = 0.9965$, where the moisture content is

$$X = \frac{\varepsilon_\beta \cdot \rho_\beta}{\varepsilon_\sigma \cdot \rho_\sigma} \tag{16}$$

The $P_{vs(T_\sigma)}$ is calculated by using the equation from ASHRAE Fundamentals 6.2, 2001.

To theoretically model and numerically simulate this head and mass transfer process, the governing equations are listed here [8,11]:

Aqueous adsorbed phase continuity equation:

$$\frac{\partial \varepsilon_\beta}{\partial t} - \dot{r}_v \Omega_\beta = 0 \tag{17}$$

where

$$\Omega_\beta = 1/\rho_\beta \tag{18}$$

Momentum equation:

$$U_D = -\frac{K}{\mu} \cdot \frac{\partial P}{\partial x} \tag{19}$$

Gas energy equation:

$$\frac{\partial(\varepsilon_\gamma \rho_\gamma c_{pa} T_\gamma)}{\partial t} + \frac{\partial(\rho_\gamma U_D c_{pa} T_\gamma)}{\partial x} = \frac{\partial}{\partial x}\left(k_{\gamma,\mathrm{eff}} \frac{\partial T_\gamma}{\partial x}\right) + h_{\sigma\gamma} S_v (T_\sigma - T_\gamma) \tag{20}$$

where

$$k_{\gamma,\mathrm{eff}} = \varepsilon_\gamma(\rho_a k_a + \rho_v k_v)/(\rho_a + \rho_v) \tag{21}$$

$$h_{\sigma\gamma} = J_h \cdot c_{pa} \cdot G_\gamma / Pr^{2/3} \tag{22}$$

where

$$J_h = 0.052 Re^{-0.3} \tag{23}$$

Adsorbed liquid and solid energy equation:

$$\frac{\partial((1-\varepsilon_\gamma)\rho_{\sigma\beta} c_{p(\sigma\beta)} T_\sigma)}{\partial t} = \frac{\partial}{\partial x}\left((1-\varepsilon_\gamma) k_{\sigma,\mathrm{eff}} \frac{\partial T_\sigma}{\partial x}\right) + (1-\varepsilon_\gamma)\dot{r}_v Q - h_{\sigma\gamma} S_v (T_\sigma - T_\gamma) \tag{24}$$

where

$$\rho_{\sigma\beta} = (\varepsilon_\sigma \rho_\sigma + \varepsilon_\beta \rho_\beta)/\varepsilon_\sigma + \varepsilon_\beta \tag{25}$$

$$c_{p(\sigma\beta)} = (\varepsilon_\sigma c_{p(\sigma)} + \varepsilon_\beta c_{p(\beta)})/\varepsilon_\sigma + \varepsilon_\beta \tag{26}$$

$$k_{\sigma,\mathrm{eff}} = (\varepsilon_\sigma k_\sigma + \varepsilon_\beta k_\beta)/(\varepsilon_\sigma + \varepsilon_\beta) \tag{27}$$

$$Q = CH_{fg} \tag{28}$$

The values of the coefficient C in Eq. (28) for different simulation test conditions has been found to be dependent on the moisture content and partly on the inlet air humidity [8].

Water vapour mass diffusion equation:

$$\frac{\partial(\varepsilon_\gamma \rho_a W_v)}{\partial t} + \frac{\partial(\rho_a U_D W_v)}{\partial x} = \frac{\partial}{\partial x}\left(\rho_a D_{v,\mathrm{eff}} \frac{\partial W_v}{\partial x}\right) - \dot{r}_v \tag{29}$$

where

$$D_{v,\mathrm{eff}} = D_v \cdot \varepsilon_\gamma/\tau \tag{30}$$

The volumetric constraint on the volume fractions requires that:

$$\varepsilon_\gamma + \varepsilon_\beta + \varepsilon_\sigma = 1 \tag{31}$$

The accompanying thermodynamic relations used are:

$$P_v = \rho_v R_v T_\gamma \tag{32}$$

$$P_a = P - P_v \tag{33}$$

$$\rho_a = P_a/R_a T_\gamma \tag{34}$$

$$\rho_v = \rho_a W_v \tag{35}$$

$$\rho_\gamma = \rho_a + \rho_v \tag{36}$$

Initially the bed temperature is uniform

$$t = 0: \quad T_\gamma = T_\sigma = T_0 \tag{37}$$

Initially, the silica gel sample is assumed to be dry

$$t = 0: \quad W_v = W_{v0} = 0, \quad X = X_0 = 0 \tag{38}$$

The inlet conditions are

$$x = 0: \quad T_\gamma = T_\infty, \quad \frac{\partial T_\sigma}{\partial x} = 0, \quad W_v = W_{v\infty} \tag{39}$$

The outlet conditions are

$$x = L: \quad \frac{\partial T_\gamma}{\partial x} = 0, \quad \frac{\partial T_\sigma}{\partial x} = 0, \quad \frac{\partial W_v}{\partial x} = 0 \tag{40}$$

The set of coupled, nonlinear, partial differential equations above were discretized by using the finite volume (control volume) method [12]. The implicit scheme was applied everywhere. A central difference scheme was used for the convection term discretization of the gas energy equation and an up-wind scheme was for the water vapour diffusion equation. The equations were solved using the Gauss–Seidel method. A time step of 0.01 s with total time step of 10 h and a grid mesh of 0.1 mm with total 80 grid points were used in the simulation to ensure numerical stability and accuracy. While the grid was equal to or smaller then 0.1 mm, the simulation results were independent of the grid value selection. The pressure drop through the silica gel bed was obtained from the Darcy equation, and the Darcy velocity was considered to be constant and a known variable.

The numerical procedure started from the parameters definition and initialization. Based on the initial and the boundary values of temperatures, relative humidity, moisture content, the volume fraction of gas (ε_γ) was obtained from the volumetric constraint equation; the dry air, water vapour pressure (P_v, P_a) and density of gas, water vapour, dry air ($\rho_\gamma, \rho_v, \rho_a$) were calculated by thermodynamic equations of state. Then, the water vapour adsorption rate ($\dot{r}$) was solved and finally the volume fraction of adsorbed water (ε_β) was obtained through the aqueous phase continuity equation. When the unknown variables ε_β, ε_γ, ρ_γ, ρ_v, ρ_a, P_v, P_a and $\dot{r}_v$ were determined, they were used three main differential equations to obtain dependent variables, T_γ, T_σ and W_v. Since the Gauss–Seidel iteration method was used, the source terms and main dependent variables, T_γ, T_σ, W_v, were updated to make the program converge quickly. When calculations at all the grid points were done, and the maximum difference between the current values and those of the previous iteration for T_γ, T_σ and W_v was less than 10^{-6}, the program went to the next time step until the termination time was reached.

The properties of the silica gel samples used in this simulation were: the particle density $\rho_s = 2400\ \text{kg/m}^3$, heat capacity $c_{ps} = 700\ \text{J/kg K}$, other properties are listed in Table 1.

3. Test facility and procedure

The test facility used a forced convection humid air flow to pass an initial dry silica gel particle bed, as shown in Fig. 1. This facility was designed to result in one-dimensional heat and mass transfer with constant or steady state inlet boundary conditions after the start. The Darcy velocity in the test section was 0.0708 m/s, and $Re = 0.374$. Nine thermocouples (bias ± 0.667 K) were mounted in the 0.08 m deep sample bed, with one (T b1) well above the sample, one (T b2) on the top of the bed surface, three (T b3 to T b5) evenly situated between the top and the bottom, and another three (T b6 to T b8) were horizontally distributed over the bottom of the sample bed adjacent to the fibre glass support, a 0.03 mm thick permeable board. The maximum difference in temperature for the three thermocouples at the outlet was less than 2.5 K during all experiments. Two relative humidity sensors were placed 0.05 m up stream from the inlet duct (RH 1) and 0.5 m down stream from the outlet duct (RH 2) respectively. They measured the inlet and outlet air bulk relative humidities with bias $\pm 1.2\%$. Precision for temperature and RH measurement were negligible compared to these biases.

Before starting each experiment, the silica gel sample was dried in an oven at 393 K for 12 h. After cooling to room temperature, the dry silica gel sample of about 1 kg was poured into the test section with thermocouples carefully placed in designed locations. The test section was then installed in the environment chamber which was preconditioned to the required temperature and relative humidity. During the experiment, the pressure drop was held to obtain a constant mass flow rate of air and the silica gel sample undergone a transient adsorption process. The initial temperature of the sample was the chamber air temperature, and the humidity ratio in test sample was nearly zero. After an experiment started, a steady moist air flow at certain temperature, humidity, and air flow rate passed through the test section. A fraction of the water vapour was then adsorbed

Table 1
The properties of the silica gel samples used in the simulation

	$d_p = 1.0$ mm (Particle size distribution from 14 to 20 mesh)	$d_p = 2.0$ mm (Particle size distribution from 6 to 12 mesh)
K (m^2)	3.94×10^{-10}	6.6×10^{-10}
ε	0.629	0.631
S_{v0} (m^2/m^3)	2.0×10^3	1.5×10^4
S_{v1} (m^2/m^3)	1.0×10^3	1.0×10^4
t_0 (h)	0.8	1.2

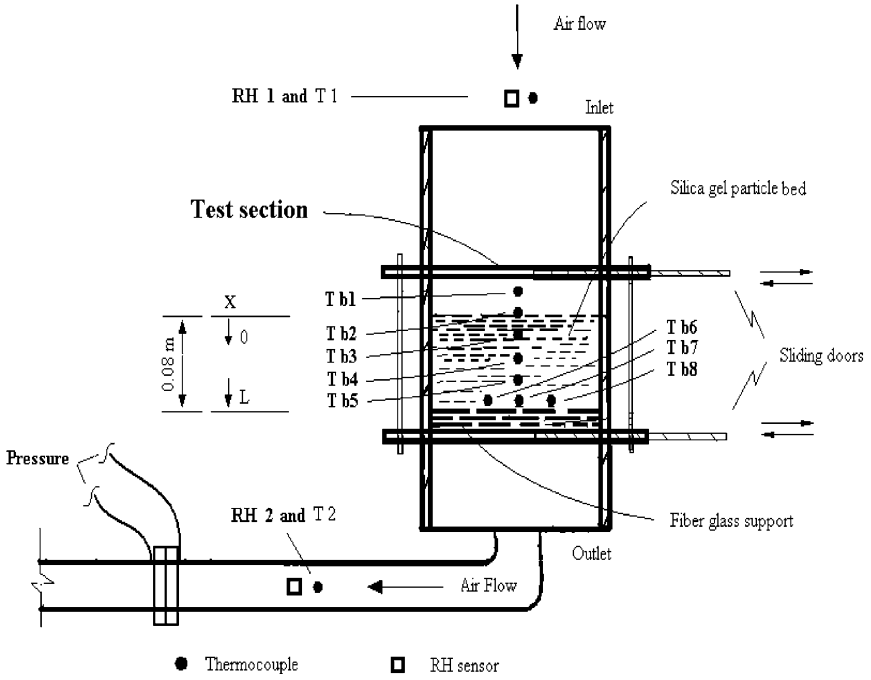

Fig. 1. Experimental facility.

on the surfaces of granular silica gel particles. The sensible energy changes were partly carried downstream by the air flow, causing the air temperature first to rise and later to fall at the outlet side.

4. Results and discussion

A constant 295 K inlet air temperature was used for experiments. Three different values of inlet humidity (50%, 70%, 90%) were tested. Two sizes of silica gel particles (average size $d_p = 1.0$ and 2.0 mm) were tested for the three relative humidities respectively. The numerical simulation results of the temporal and spatial variation in temperature, relative humidity and moisture content in the silica gel sample bed were compared with the corresponding measured values. Each test was performed for 10 h. The uncertainties presented did not include the inlet starting conditions and the impact of the different moisture adsorption of different samples on the measured results. To clearly show all the uncertainties in the experimental points, some of the uncertainty bars were shifted.

Fig. 2 shows the bed temperature versus position in the test section at different times. Initially, the temperature was uniform everywhere and equal to the chamber temperature. After the flow started, the heat generated due to adsorption of water vapour caused the bed temperature to first increase rapidly, except at the inlet, and then to decrease. Fig. 3 shows the simulated interstitial relative humidities of air within the sample bed for the same test conditions as Fig. 2. Shortly after a test started, the outlet humidity dropped to a minimum, then rise toward the inlet relative humidity. This simulation shows that over time, less water vapour was lost from the inlet air. However, even at 10 h some moisture was still adsorbed in the bed. The numerical simulation of spatial variation of moisture content of the particles in the bed is shown in Fig. 4 for the same test conditions. When a test started, the particles close to the inlet of test section rapidly adsorbed water vapour from the air, the moisture content of these particles quickly rise towards their saturation state. The equilibrium moisture content of silica gel particles was measured in separate tests. Fig. 5 shows the equilibrium moisture content of silica gel particles ($d_p = 1$ mm) subject to different relative humidity conditions where each data point required a 48-h test. The uncertainty bars were based on three tests for each relative humidity, implying significant sample variations or uncertainties, especially at high humidities. Comparisons between Figs. 4 and 5 suggested that even after 10 h of testing for Fig. 4, the silica gel still retained a significant capacity for moisture adsorption. The temporal temperature comparison, presented in Fig. 6, shows that the numerical results appear to be in the best agreement with the experimental data for short time periods before the temperature peaks were reached; however, even for large times the simulations were gen-

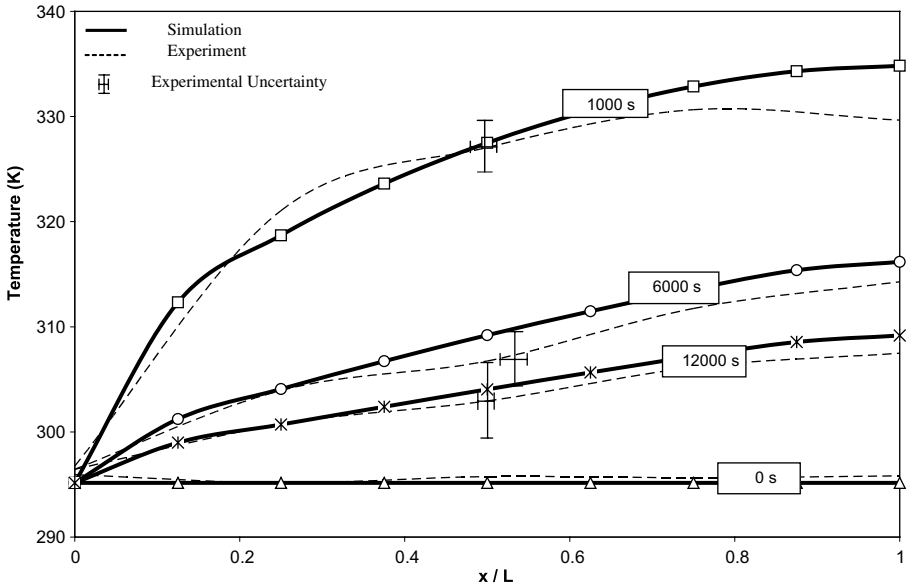

Fig. 2. Simulated and experimental temperatures versus position for $d_p \cong 2$ mm, $U_D = 0.0708$ m/s, $T_\infty = 295.15$ K, $RH_\infty = 70\%$.

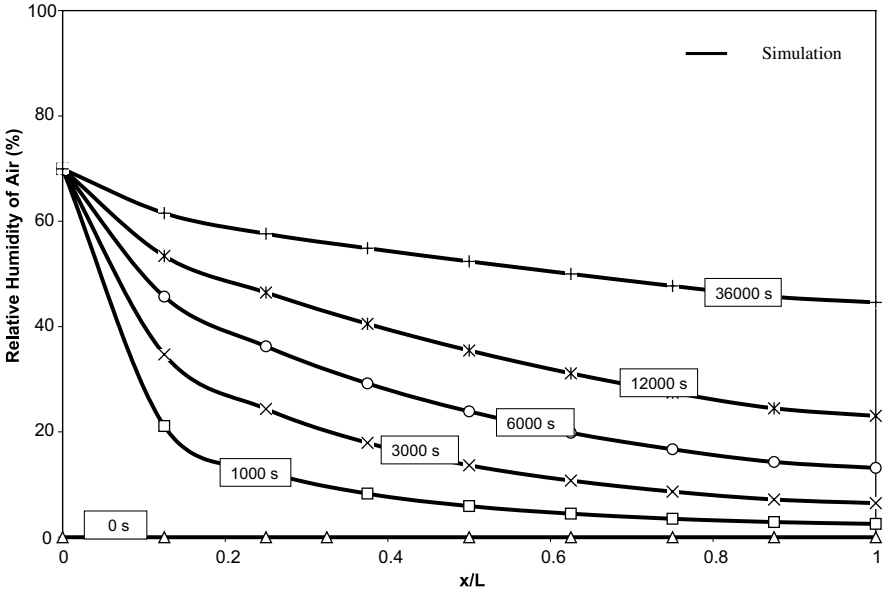

Fig. 3. Simulated relative humidities versus position for $d_p \cong 2$ mm, $U_D = 0.0708$ m/s, $T_\infty = 295.15$ K, $RH_\infty = 70\%$.

erally within the experimental uncertainty bounds. In part, these discrepancies may be due to variations between moisture adsorption characteristics for various samples as implied in Fig. 5. Fig. 7 is temporal relative humidity comparisons of numerical results and experimental data. As discussed in the analysis of the temperature response, the parameter values used in the numerical model may cause the simulation results to differ from the experimental data. The experimental location of the RH sensors is another reason for uncertainties since numerically the inlet and outlet RH strictly meant the RH of top and bottom of the sample bed while experimentally it was not the case.

Uncertainties in the value of silica gel properties cause bias uncertainties in the simulation results. Among them, the specific surface area (S_v) has the biggest effect

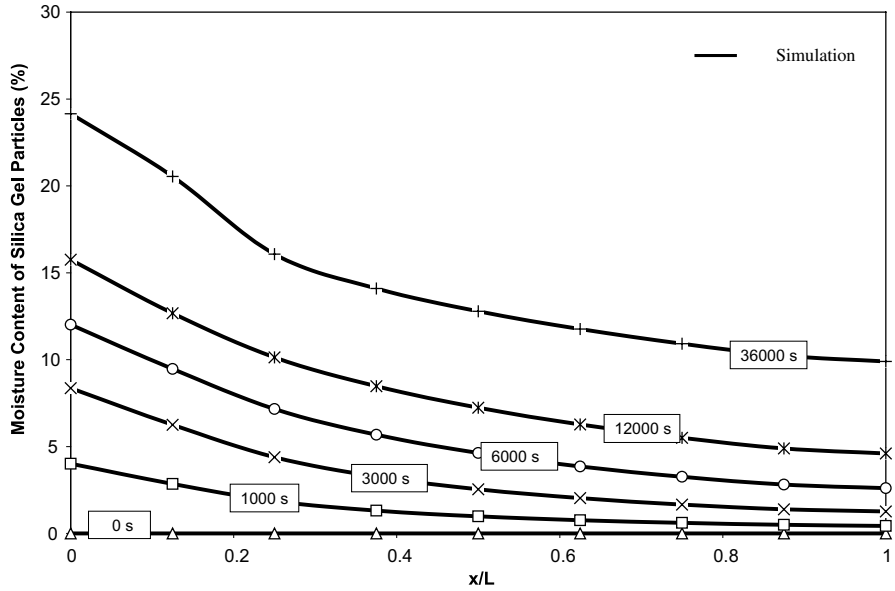

Fig. 4. Simulated moisture content versus position for $d_p \cong 2$ mm, $U_D = 0.0708$ m/s, $T_\infty = 295.15$ K, $RH_\infty = 70\%$.

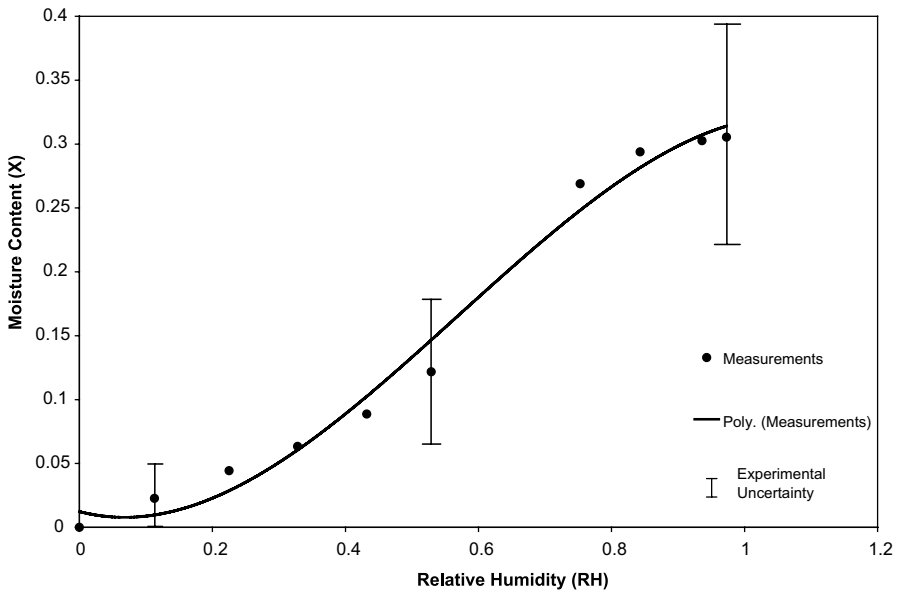

Fig. 5. Equilibrium moisture content as a function of relative humidity at room temperature (295.15 K) for silica gel particles ($d_p \cong 1$ mm).

on the results. Using simulation parameter studies of S_v, it was evident from comparisons with the experimental data that the specific surface area available for moisture accumulation was not constant in time. More adsorption surface area became available for moisture adsorption in the bed than was initially available. Furthermore this apparent added surface area for adsorption increased rapidly at first as implied by a transient response to a step change. This observation is consistent with the specific surface area studies for particulate desiccant materials such as silica gel which are reported by the silica gel supplier to have a very large internal specific surface area. As well, the external surface area of particles using the Carman correlation [13] is much smaller.

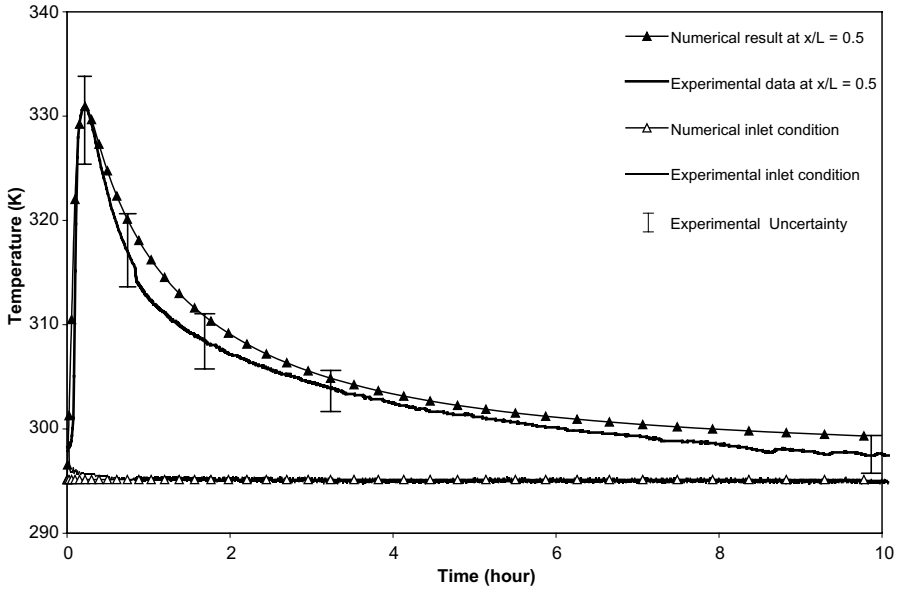

Fig. 6. Numerical and experimental temperatures versus time for $d_p \cong 1$ mm, $U_D = 0.0708$ m/s, $T_\infty = 295.15$ K, $RH_\infty = 70\%$, $x/L = 0$ and 0.5.

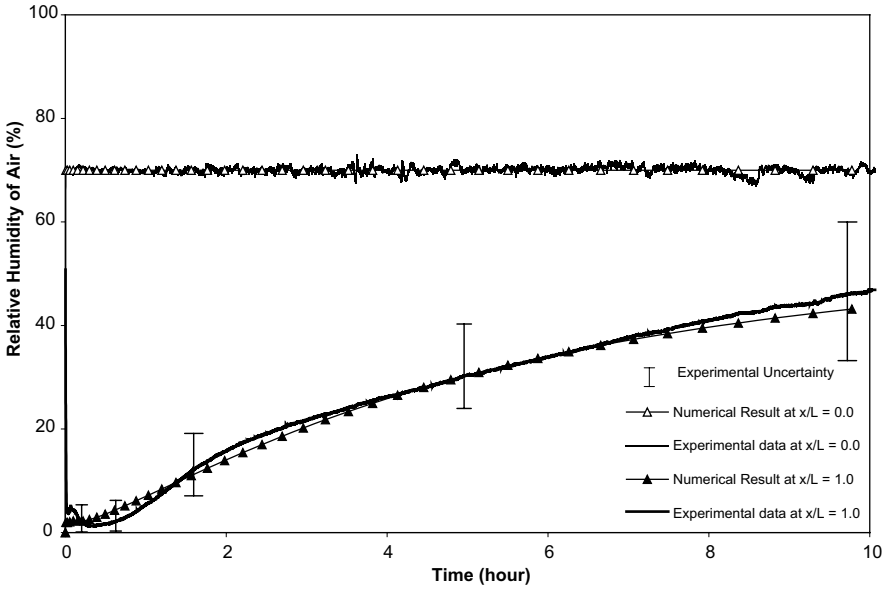

Fig. 7. Simulated and experimental relative humidities versus time for $d_p \cong 1$ mm, $U_D = 0.0708$ m/s, $T_\infty = 295.15$ K, $RH_\infty = 70\%$.

Therefore it is expected that the amount of surface area available for moisture adsorption inside each particle is limited by a diffusion process inside each particle while the surface area at time zero for a transient process is a small fraction of the total internal area. The theoretical model of this time varying specific surface area used in the analysis is given by Eq. (8), $S_v = S_{v0} + S_{v1}(1 - e^{-t/t_0})$.

Different size particles have different moisture adsorption capacity. The small size silica gel particles ($d_p = 1$ mm) always released more heat per unit volume compared to the larger size silica gel particles ($d_p = 2$ mm), at same inlet conditions. This verifies that small particles have more specific surface area available at any time and have a stronger ability to adsorb moisture and release heat.

5. Summary and conclusions

In this study, the one-dimensional, transient, non-equilibrium heat transfer and moisture diffusion within the silica gel particle bed were investigated numerically and experimentally. The coupled nonlinear particle differential equations were solved by finite control method. The results show that: as a desiccant, silica gel particles have very high moisture adsorption capacity and may adsorb moisture up to one-third of each particle's dry mass, the inlet humid air flow passing through a silica gel bed causes a significant temperature rise and humidity decrease in the exhaust air.

Although silica gel particles have a large specific surface area, there is a long time delay in the temperature and humidity response of silica gel bed during moisture adsorptions when particles of 1 or 2 mm in diameter were used (e.g. time constants of 10 h were indicated in this study).

This finding implies that the internal specific surface area of particles is only exposed to water vapour gradually over an extended time and that this time delay must be accounted for in the model development for any transient tests with even small particles. The size of the silica gel particles is important for the transient response of temperature and humidity. For the same test condition and the same volume of the particle bed, smaller sized particles with larger total specific surface area adsorb more moisture and therefore release more heat than bigger particles. The comparison of numerical results and experimental data was well within the uncertainty range. That supports that the theoretical analysis of the heat and mass transfer in the silica gel is correct and will give accurate prediction.

References

[1] R.W. Besant, C. Simonson, Air-to-air exchangers, ASHRAE J. 45 (4) (2003) 42–52.
[2] A.A. Pesaran, A.F. Mills, Moisture transport in silica gel packed beds—I. Theoretical study, Int. J. Heat Mass Transfer 30 (1987) 1037–1049.
[3] D.M. Ruthven, Principles of Adsorption and Adsorption Processes, A Wiley-Interscience Publication, 1984, pp. 5–26.
[4] J.-Y. San, G.-D. Jiang, Modeling and testing of a silica gel packed-bed system, Int. J. Heat Mass Transfer 37 (8) (1994) 1173–1179.
[5] Y. Fujii, N. Lior, Conjugate heat and mass transfer in a desiccant-airflow system: a numerical solution method, Numer. Heat Transfer, Part A: Applications 29 (7) (1996) 689–706.
[6] H.S. Al-Sharqawi, Noam Lior, Conjugate computation of transient flow and heat and mass transfer between humid air and desiccant plates and channels, Amer. Soc. Mech. Engnrs., Heat Transfer Div. (Publication) HTD 374 (4) (2003) 263–275.
[7] C.-C. Ni, J.-Y. San, Mass diffusion in a spherical microporous particle with thermal effect and gas-side mass transfer resistance, Int. J. Heat Mass Transfer 43 (2000) 2129–2139.
[8] S. Peng, R.W. Besant, G. Strathdee, Heat and mass transfer in granular potash fertilizer with a surface dissolution reaction, Can. J. Chem. Eng. 78 (2000) 1076–1086.
[9] F.M. White, Heat Transfer, Addison-Wesley Publishing Company, Inc., 1984.
[10] S.J. Gregg, K.S.W. Sing, Adsorption, Surface Area and Porosity, second ed., Academic Press, 1982.
[11] M. Kaviany, Principles of Heat Transfer in Porous Media, second ed., Springer, 1995.
[12] Patankar, Numerical Heat Transfer and Fluid Flow, Hemisphere Publishing Corporation, McGraw-Hill Book Company, 1980.
[13] P.C. Carman, The determination of the specific surface. I, J. Soc. Chem. Eng. 2 (1938) 225–234.